Eur. J. Mech., B/Fluids, **16**, n° 6, 761-778, 1997

Global modes in falling capillary jets

S. LE DIZÈS *

ABSTRACT. – The global linear stability analysis of falling capillary jets is carried out when the density of ambient gas is negligible. The jet is assumed to be dominated by inertia (*i.e.* $\mathrm{Re} = R_0 U_0/\nu \gg 1$ and $\varepsilon = gR_0/U_0^2 \ll 1$, where g is the gravity, R_0 and U_0 are the radius and the speed of the jet at the orifice, ν the viscosity of the liquid) so that it evolves on a larger scale than Rayleigh instability wavelengths. If the basic jet is approximately an axisymmetric plug profile in each section, it becomes locally absolutely unstable at the orifice for a critical value $W_a \approx 0.32$ of the Weber number $W_0 = \gamma/\rho R_0 U_0^2$ where γ is the surface tension between the liquid and the gas, and ρ the liquid density. Just above that value, it is demonstrated that there exists a discrete number of unstable global modes, *i.e.* time-harmonic perturbations satisfying homogeneous boundary conditions at the orifice and causal conditions at infinity. These modes differ from the Airy-type global modes obtained by Monkewitz *et al.* (1993): They are composed of three spatial branches interacting at the orifice. The critical Weber number for the global transition is obtained as a function of ε and Re. It is computed for the jet of water in air for Reynolds numbers ranging from 100 to 200, and compared to experimental data for the transition to dripping. The conjecture by Monkewitz (1990) that the transition to dripping could be related to a global instability is discussed in light of these results.

1. Introduction

Falling capillary jets are known to break up into drops at a distance from the orifice that varies with the flow rate and disturbance level. As the flow rate is decreased, the breakup comes closer to the orifice and the jet eventually exhibits a transition to dripping, *i.e.* drops form at the orifice. Monkewitz (1990) conjectured that this transition could be related to a global linear instability of the basic jet. The goal of this article is to justify this interpretation by calculating the global stability characteristics of a falling capillary jet.

So far, stability analyses have mostly focused on homogeneous jets. The temporal stability properties of a plug profile have been calculated by Rayleigh (1878) in the non-viscous regime and by Chandrasekhar (1961) in the viscous regime. Leib and Goldstein (1986a, b) have considered the impulse response problem and determined the absolute/convective nature of the instability (Bers, 1983; Huerre and Monkewitz, 1990) for the definition of absolute and convective instabilities). They have proved that plug profiles exhibit a transition to absolute instability as the flow rate is decreased in both viscous and non-viscous regime. Yakubenko (1997a) focused on the role played by the boundaries. He analysed the instability generated by the wave reflections at the boundaries of a long but finite jet.

The results for homogeneous jets can be applied to a spatially-evolving jet if the spatial evolution scale is much larger than typical instability wavelengths. Indeed, they allow

* Institut de Recherche sur les Phénomènes Hors Équilibre, 12, avenue du Général Leclerc, 13003 Marseille, France.

0997-7546/97/06/$ 7.00/

definition of *local* stability properties at each position, and consequently a classification of each flow according to the nature of the loca behavior. Such a classification has been very successful in shear flow (Huerre and Monkewitz, 1990; Monkewitz, 1990). The link between the local stability properties and the global behaior of the flow has been the subject of numerous studies but is still not clear. Neverheless, most observations support the idea that flows that are locally convectively unstable everywhere, are in general strong noise amplifiers while flows with a region of local absolute instability can exhibit intrinsic global dynamics.

From the stability results for homogeneous jets, falling capillary jets are found to be at least convectively unstable everywhere. Below a critical flow rate, they become absolutely unstable in the neighborhood of the orifice, and then could be subject to a global instability.

Global instability is in general studied by considering global modes, *i.e.* linear time-harmonic perturbations of the entire flow subject to boundary conditions. As soon as there exists a global mode frequency ω_g of positive growth rate $\Im m\,(\omega_g) > 0$, the basic flow is considered as globally unstable. The weak inhomogeneity assumption allows a global mode description in the WKBJ framework (Huerre and Monkewitz, 1990). In the that framework, the spatial structure of the global modes is prescribed at leading order by the local dispersion relation that defines the local stability properties. The spatial branches of the local dispersion relation give the wavenumbers of the local plane waves that approximate the global mode. As long as these spatial branches are distinct, there is no wave interaction: the global mode is then a sum of local plane wave approximations (WKBJ approximations). At the turning points where waves interact, the local plane wave approximation breaks down, and a specific local approximation describing the wave interactions has to be developed. The local plane wave decomposition of the global modes is prescribed at the flow boundaries (in particular at infinity) by the boundary conditions. In principle, the full global mode problem is then to determined the (global) frequencies for which the wave interactions are in agreement with the prescribed wave decomposition at the flow boundaries.

The very few rigorous results on global instability have been obtained when the local dispersion relation is particularly simple and reduces to a single temporal branch with two spatial branches. In such a case, the global dynamics is governed by a Ginzburg-Landau equation (GLE) in the direction of propagation of the local perturbations. Global modes have been analysed in both semi-infinite and double-infinite domains. But it is only in double-infinite domains that a general characterisation of the most unstable global modes has been obtained (Chomaz *et al.*, 1991; Le Dizès *et al.*, 1996; Le Dizès, 1997). In semi-infinite domains, such a characterisation is not available without additional assumptions concerning the local stability properties (Chomaz *et al.*, 1988).

For falling capillary jets, it seems more appropriate to work in a semi-infinite domain, and to impose homogeneous boundary conditions on one side (the orifice). In such a configuration but in a different context, Monkewitz *et al.* (1993) have obtained a frequency selection criterion which states that the complex frequencies of the most unstable global modes are given at leading order by the local absolute frequency at the

boundary. The analysis of global modes in falling capillary jets is similar in many ways to the analysis developed in Monkewitz *et al.* (1993). To clarify that study, it is useful briefly to review the results and underlying assumptions of Monkewitz *et al.* (1993). The global modes obtained in Monkewitz *et al.* (1993) admit two distinct approximations: far from the boundary (in a so-called Outer Region), each global mode is a local plane wave propagating to the right as prescribed by causality (Kulikovskii, 1985); close to the boundary (in a Inner Region), it is Airy function describing the interaction at a turning point of two waves propagating in opposite directions. The frequencies of the global modes are selected by the condition of matching of Inner and Outer solutions. In Monkewitz *et al.* (1993) analysis, the full global mode problem is then reduced to a *local eigenvalue problem* in the Inner region. The physical consequence is that global modes are governed by a small region near the boundary which plays the role of an oscillating source for the whole flow. The conditions of validity of Monkewitz *et al.* (1993)'s frequency selection criterion have not been discussed so far. But it is clear that they would require that wave interactions are exclusively between two waves propagating in opposite directions and that these interactions occur only close to the boundary. It is interesting to note that these two conditions are satisfied in the GLE framework if the most unstable regions are close to the boundary.

Yakubenko (1997b) recently analysed the global mode problem for an inclined capillary jet. He obtained the surprising result that the jet could become globally unstable without any locally absolutely unstable region. In this analysis, the unstable global modes are composed of three waves which interact at several points in the flow.

For falling capillary jets, the most unstable regions are close to the boundary, so we expect wave interactions to be localised near the orifice as in Monkewitz *et al.* (1993) and not as in Yakubenko (1997b). But, the wave interactions can not be limited to two waves since the third wave that intervenes in Yakubenko's analysis is also present. The goal of this paper is to show that, despite that third wave, there still exist global modes whose frequencies are given at leading order by the local absolute frequency at the orifice.

The paper is organized as follows. In section 2, the falling capillary jet model is presented. Section 3 is concerned with the reduction of the global mode problem to a local eigenvalue problem near the orifice. The three waves that compose the global mode are studied in the Outer region far from the orifice in section 3.1, while the interaction process in the Inner region near the orifice is analysed in section 3.2. The local eigenvalue problem is solved in the Appendix. The results are presented in section 4, first in a general setting (section 4.1), then in the case of a jet of water in air (section 4.2). In particular, the critical curve for the global transition is drawn and compared to experimental data for the transition to dripping. Section 5 briefly summarizes the main results and discusses the link between global instability and the transition to dripping.

2. Basic flow and local dispersion relation

Consider an incompressible liquid with surface tension and viscosity falling from a circular exit under the force of gravity into an ambient gas of negligible density. This

falling capillary jet is controlled by three parameters, the Weber number $W_0 = \gamma/\rho R_0 U_0^2$, the Reynolds number $\mathrm{Re} = R_0 U_0/\nu$ and the Froude number $F = U_0/\sqrt{gR_0}$ where γ is the surface tension between the liquid and the gas, ρ and ν the density and the viscosity of the liquid, U_0 the velocity of the liquid at the orifice, and R_0 the radius of the orifice. The jet is assumed to be dominated by inertia such that both Re and F are considered large below.

If all velocities and distances are non-dimensionalized with respect to U_0 and R_0 respectively, a simple approximation for the basic jet can be derived: at leading order, the velocity remains oriented along the vertical direction and uniform in each section while it slowly evolves with respect to the downstream coordinate $X = \varepsilon x$ where ε is a small parameter related to the Froude number through $\varepsilon = 1/F^2 = gR_0/U_0^2$. The x-axis is chosen to be oriented downstream and $x = 0$ is the orifice. If one denotes by $U(X, W_0)$ the velocity of the jet at a streamwise station X, the (non-dimensionalized) radius of the jet evolves according to $R(X, W_0) = 1/\sqrt{U(X, W_0)}$ and the local Weber number formed with these quantities is related to W_0 through $W(X, W_0) = W_0/[U(X, W_0)]^{3/2}$. As the velocity $U(X, W_0)$ increases downstream, the local Weber number W decreases and the jet becomes locally more and more stable.

The most unstable local modes are axisymmetric. Their frequency ω and wavenumber k are linked by a local dispersion relation $D(\omega, k, X, W_0, \mathrm{Re}, \varepsilon) = 0$ which can be expanded for large Reynolds numbers and small ε as

$$D(\omega, k, X, W_0, \mathrm{Re}, \varepsilon) = D_0(\omega, k, X, W_0) + \frac{1}{\mathrm{Re}} D_1(\omega, k, X, W_0) + O(\mathrm{Re}^{-3/2}, \varepsilon). \tag{1}$$

The leading order term D_0 has been derived by Rayleigh (1878):

$$D_0(\omega, k, X, W_0) = -(\Omega - K)^2 + W(K^2 - 1) K \frac{\mathbf{I}_1(K)}{\mathbf{I}_0(K)}, \tag{2}$$

where $\mathbf{I}_0$ and $\mathbf{I}_1$ are the usual Bessel functions and

$$K = k/\sqrt{U(X, W_0)}, \tag{3a}$$

$$\Omega = \omega/[U(X, W_0)]^{3/2}, \tag{3b}$$

$$W = W_0/[U_0(X, W_0)]^{3/2}. \tag{3c}$$

The first correction term D_1 is obtained by expanding Chandrasekhar's dispersion relation (Chandrasekhar, 1961):

$$D_1(\omega, k, X, W_0) = 2iK^2 \left(-WK(K^2 - 1) \frac{\mathbf{I}_1(K)}{\mathbf{I}_0(K)(\Omega - K)} + \frac{\mathbf{I}_1'(K)}{\mathbf{I}_0(K)} (\Omega - K) \right). \tag{4}$$

Note that the spatial dependency in (2) and (4) only appears through the velocity $U(X, W_0)$ in the rescaled variables $(3a, b, c)$.

The local dispersion relation defines the local stability properties of the jet: the jet is locally unstable for any positive Weber number and becomes locally absolutely unstable for Weber numbers above the (non-viscous) critical value $W_a \approx 0.32$ (Leib and Goldstein, 1986a). For a Weber number W_0 just above the critical value W_a, the jet is then locally absolutely unstable in a small neighbourhood near the orifice and convectively unstable everywhere else.

Guided by the analysis of Monkewitz *et al.* (1993), we look for the global frequencies close to the local absolute frequency $\omega_0(0, W_0)$ at the orifice. The Weber number W_0 will be chosen close to the critical value W_a such that the possible global modes are almost neutral. As explained in the introduction, these global modes are expected almost everywhere to be a sum of non-interacting local plane waves whose characteristics are given by the local dispersion relation, *i.e.* at leading order by $D_0(\omega_o^a, k, X, W_a) = 0$ where $\omega_o^a = \omega_0(0, W_a)$. By definition of the local absolute frequency, two waves propagating in opposite directions interact at the orifice. These two waves have a local wavenumber k_o^a that satisfies

$$\frac{\partial \omega}{\partial k}(k_o^a, 0, W_a) = 0 \tag{5}$$

where $\omega(k, X, W_o)$ is one of the two temporal branches of $D_0(\omega, k, X, W_o) = 0$. One can easily check that k_o^a also satisfies $\partial_k^2 \omega(k_o^a, W_a, 0) = 0$ and $\partial_k^3 \omega(k_o^a, W_a, 0) \neq 0$ which means that a third wave is present in the interaction process near the orifice.

The goal of this article is to prove that these three waves can form a global mode.

3. Three-waves global modes

The behavior of the three waves is first considered in the Outer region. The direction of propagation of each wave is determined and it is checked that the three waves do not interact far from the orifice. The interaction process between the three waves is studied afterwards. It leads to a local eigenvalue problem for the global frequencies.

3.1. Outer region

For a frequency and a Weber number given at leading order by ω_o^a and W_a respectively, the local spatial branches obtained from the local dispersion relation move in the complex k-plane as one goes downstream due to the increase of $U(X, W_0)$. The trajectories in the complex k-plane of the three spatial branches that pinch at the orifice are shown in Figure 1.

The three wavenumbers have distinct imaginary parts for all positive X. This property guarantees that there is no interaction between these wavenumbers away from the orifice. Assuming that there is no interaction with other waves, the local plane wave approximation associated with these wavenumbers are uniformly valid in the Outer region.

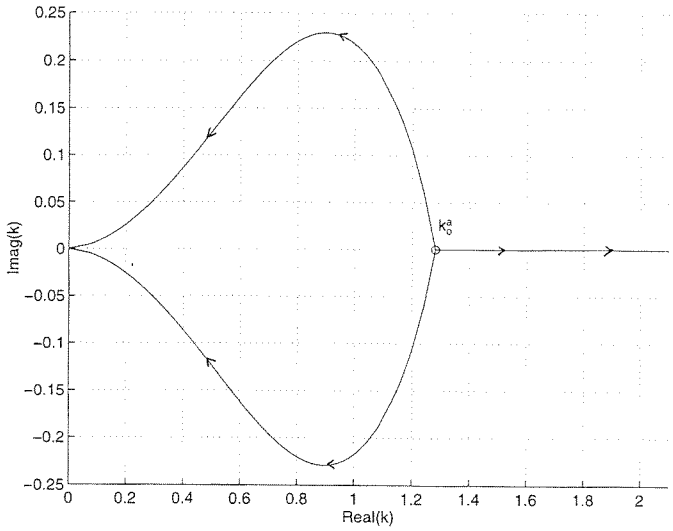

Fig. 1. – Trajectories in the complex k-plane, as X varies, of the non-viscous local wavenumbers for $W_0 = W_a$ and $\omega = \omega_o^a$. Only the three branches that pinch at the orifice at k_o^a are represented. The arrows indicate the direction of variation as X increases.

They exhibit the three possible behaviors in the downstream direction: one is exponentially increasing ($\Im m\ (k) < 0$), another is exponentially decreasing ($\Im m\ (k) > 0$) and the last one is oscillatory ($\Im m\ (k) = 0$).

Causality selects the waves which are allowed in the Outer region (*see* Bers, 1983; Kulikovskii, 1985). Since the jet is absolutely stable in the Outer region, no energy can be generated at infinity by a linear mechanism, which means that all the waves must propagate to the right. In a stable medium, this condition is equivalent to allowing only decreasing wabes. In a convectively unstable medium, the selection is not as simple and one must determine precisely the direction of propagation of each wave, which is defined by the sign of $\Im m\ (k)$ for large[1] $\Im m\ (\omega)$. If $\mathrm{sgn}\,(\Im m\ (k))$ becomes positive for large $\Im m\ (\omega)$, the wave propagates to the right (downstream), if $\mathrm{sgn}\,(\Im m\ (k))$ becomes negative, it propagates to the left (upstream). Figure 2 shows the trajectories of the three branches of Figure 1 at an arbitrary fixed location $X > 0$ as $\Im m\ (\omega)$ varies.

The oscillatory wave has a negative $\Im m\ (k)$ for large $\Im m\ (\omega)$. Thus it propagates upstream. The two other wavenumbers tend to the upper complex half-plane: they therefore both propagate downstream. Accordingly, these two wavenumbers will be designated as k_1^+ and k_2^+, where k_1^+ corresponds to, say, the exponentially increasing wave ($\Im m\ (k_1^+ < 0)$. The third wavenumber will be designated as k_1^-.

If one applies causality, the waves k_1^+ and k_2^+ are then allowed in the Outer region whereas k_1^- is forbidden. In the Outer region, the global mode is therefore approximated by the sum of the two local plane waves of wavenumbers k_1^+ and k_2^+. The local plane wave approximations (WKBJ approximations) can be computed by a recursive method

[1] The sign of $\Im m\ (k)$ does not change for $\Im m\ (\omega)$ larger than the local maximum growth rate.

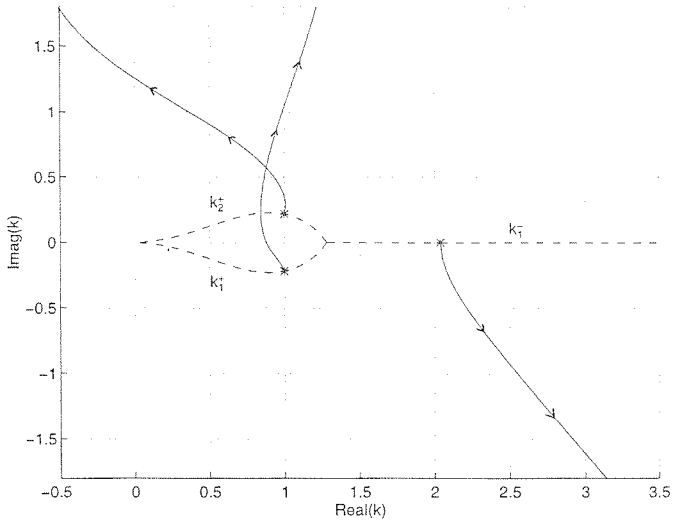

Fig. 2. – Trajectories in the complex k-plane of the three non-viscous local wavenumbers represented in Figure 1 for an arbitrary fixed X as $\Im m\,(\omega)$ is increased from zero. The wavenumbers k_1^+ and k_2^+ end in the upper half-plane for large $\Im m\,(\omega)$, while k_1^- ends in the lower half-plane.

which is explained in details in several textbooks (*see*, for instance, Bender and Orszag, 1978). The reader is also referred to Monkewitz *et al.* (1993) for the derivation of the WKBJ approximations in the global mode framework.

3.2. Inner region

In the Inner region, the Outer local plane wave approximations break down and wave interactions occur. Due to the presence of three waves in the interactions process, the inner solution is expected to be governed by a third order amplitude equation instead of the Airy equation obtained by Monkewitz *et al.* (1993). That equation, as well as the scaling leading to it, is derived by expanding the local dispersion relation (1) near the point $(\omega, k, W, X) = (\omega_o^a, k_o^a, W_a, 0)$ as

$$\omega - \omega_o^a = \nu\,(W - W_a) + i\,\frac{\eta}{\mathrm{Re}} + \xi X + \mu\,(k - k_o^a)\,(W - W_a) + \lambda\,(k - k_o^a)^3 + \cdots. \tag{6}$$

The coefficients in (6) are calculated with a standard package of algebraic calculation such as Maple. Precise values for W_a, ω_o^a and k_0^a are computed from the equations $\partial_k \omega = \partial_k^2 \omega = 0$:

$$W_a \approx 0.32025, \quad \omega_o^a \approx 0.90517, \quad k_o^a \approx 1.28108. \tag{7}$$

For the other coefficients, one obtains:

$$\begin{cases} \nu \approx -0.58690, & \eta \approx -0.68817, \quad \xi \approx 1.96551, \\ \mu \approx -1.56127, & \lambda \approx -0.53198, \end{cases} \tag{8}$$

where the following expression for the first derivative of U_0 at the orifice (Després, 1992)

$$\frac{\partial U_0}{\partial X}(0,\, W_0) = \frac{2}{2 + W_0}$$

has been used to calculate ξ.

The balance of the term $\lambda\,(k - k_o^a)^3$ with the linear term ξX yields a particular choice for the local spatial variable:

$$\overline{X} = \frac{X}{\varepsilon^{3/4}}. \tag{9}$$

It follows that ω_g and W_0 must be expanded as:

$$\omega_g \sim \omega_o^a + \sqrt{\varepsilon}\omega_2 + \varepsilon^{3/4}\omega_3, \tag{10a}$$

$$W_0 \sim W_a + \sqrt{\varepsilon}W_2 + \varepsilon^{3/4}W_3, \tag{10b}$$

and the Reynolds number Re rescaled as

$$\frac{1}{\mathrm{Re}} = \frac{\varepsilon^{3/4}}{R}. \tag{11}$$

Upon replacing k by $k_o^a - i\varepsilon^{1/4}\,\partial_{\overline{X}}$, the local dispersion relation (6) is transformed into an amplitude equation

$$\begin{aligned} &i\sqrt{\varepsilon}\,[\omega_2 - \nu W_2]\,\Psi \\ &\quad + \varepsilon^{3/4}\left[\lambda\,\frac{\partial^3}{\partial\overline{X}^3} - \mu W_2\,\frac{\partial}{\partial\overline{X}} + i\left(\omega_3 - \nu W_3 - i\,\frac{\eta}{R} - \xi\overline{X}\right)\right]\Psi = 0, \end{aligned} \tag{12}$$

where the function Ψ represents the streamwise modulation near the orifice of a local plane wave of frequency ω_g and wavenumber k_0^a, for a Weber number W_0. Equation (12) recuces at leading order to

$$\omega_2 = \nu W_2. \tag{13}$$

The next order gives

$$\frac{\partial^3\Phi}{\partial u^3} - \overline{W}_2\,\frac{\partial\Phi}{\partial u} + iu\Phi = 0, \tag{14}$$

where

$$\Phi\,(u) = \Psi\,(\overline{X}), \tag{15a}$$

$$u = b^{1/4}\left(\overline{X} - \frac{\omega_3 - \nu W_3}{\xi} + i\,\frac{\eta}{\xi R}\right). \tag{15b}$$

$$\overline{W}_2 = aW_2, \tag{15c}$$

and

$$a = \mu/(\lambda\sqrt{b}) \approx 1.5268, \tag{16a}$$

$$b = -\xi\lambda \approx 3.69470. \tag{16b}$$

In order to select a discrete number of modes, at least three boundary conditions have to be applied to solution of (14). The form of the Outer solution prescribes the behavior of the inner solution as $\overline{X}$ tends to ∞. To achieve a possible match to the Outer solution, the inner solution cannot exhibit the "balanced" behavior associated with the branch k_1^- as $\overline{X} \to +\infty$. This precludes one of the three possible behaviors for the solutions of (14) but leaves two degrees of freedom, which means that at least two homogeneous boundary conditions have to be appied at $\overline{X} = 0$. Kulikovskii (1985) has interpreted this well-posedness condition in a more general framework and explained that the number of conditions on the right and left side of a finite or infinite domain must be always equal to the number of waves propagating to the left and right respectively.

The eigenvalue problem to be solved can now be addressed as follows. One looks for a complex number u_0 such that there exists a solution of Eq. (14) satisfying the boundary conditions:

$$\Phi(u_0) = \Phi'(u_0) = 0; \tag{17a}$$

$$\Phi \underset{u\to+\infty}{\sim} a\Phi_1^+ + b\Phi_2^+ \tag{17b}$$

where Φ_1^+ and Φ_2^+ are the "dominant" and "subdominant" formal asymptotic expansions near $+\infty$ of solutions of (14). Condition (17b) is the condition of matching with the Outer solution: Φ_1^+ and Φ_2^+ correspond to the Inner expressions for the local plane waves of wavenumbers k_1^+ and k_2^+.

The eigenvalue u_0 corresponds to the value of u at the orifice $\overline{X} = 0$. According to (15b), it is then related to ω_3 and W_3 through

$$u_0 = \frac{b^{1/4}}{\xi}\left(\frac{in}{R} - \omega_3 + \nu W_3\right). \tag{18}$$

Since the parameter W_3 only modifies the real part of ω_3 according to a relation similar to (13), one can assume without loss of generality that $W_3 = 0$. Equation (18) then reduces to

$$u_0 = \frac{b^{1/4}}{\xi}\left(\frac{in}{R} - \omega_3\right). \tag{19}$$

The eigenvalue problem is solved in detail in the appendix. The results are presented in the next section.

4. Results

4.1. Global transition characteristics

The resolution of the "non-classical" eigenvalue problem (14), (17a, b) leads to a discrete number of eigenvalues u_{0_n}, which depends continuously on the parameter $\overline{W}_2 = aW_2$. According to expressions (10a), (13), (15c) and (19), to each value u_{0_n} corresponds a global frequency ω_{g_n} given by

$$\omega_{g_n} = \omega_o^a + \sqrt{\varepsilon}\nu W_2 + \varepsilon^{3/4}\omega_{3_n} + O(\varepsilon), \tag{20}$$

where

$$\omega_{3_n}(W_2, R) = i\frac{\eta}{R} - \frac{\xi}{b^{1/4}}u_{0_n}(W_2), \tag{21}$$

the Weber and Reynolds numbers being defined by

$$W_0 = W_a + \sqrt{\varepsilon}W_2 + O(\varepsilon^{3/4}), \tag{22a}$$

$$\mathrm{Re} = R/\varepsilon^{3/4}. \tag{22b}$$

Due to the negative sign of η [*see* (8)], global growth rates $\Im m(\omega_{g_n}) \sim \varepsilon^{3/4}\Im m(\omega_{3_n})$ are increasing functions of the Reynolds number for a fixed ε. We shall see below that the modification of ε with respect to Re may reverse such a variation.

For $W_2 = 0$ all the global modes are damped ($\Im m(\omega_{3_n}) < 0$) but $\Im m(\omega_{3_n})$ increases with W_2. For a infinite Reynolds number, this evolution is shown in Figure 3.

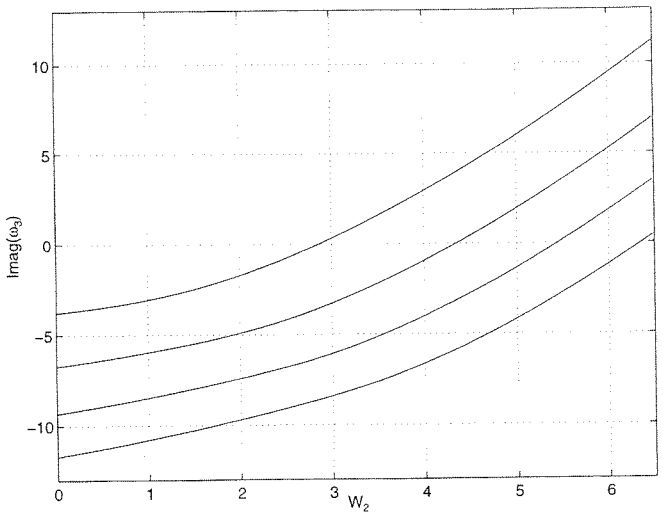

Fig. 3. – The (rescaled) global growth rates $\Im m[\omega_{3_n}]$, $n = 1, 2, 3, 4$ versus the parameter W_2 for an infinite Reynolds number.

The nth mode is destabilised at a critical value $W_{2_n}(R)$ which is obtained from $\Im m\,[\omega_{3_n}(W_{2_n}, R)] = 0$. Table I displays the first critical values together with the growth rates of the first modes for an infinite Reynolds number.

TABLE I. – Critical values of W_2 and associated growth rates of the first global modes for an infinite Reynolds number.

	W_{2_1}	W_{2_2}	W_{2_3}	W_{2_4}
	2.8632	4.3495	5.4481	6.3604
$\Im m\,(\omega_{3_1})$	0	3.9425	7.4715	10.7375
$\Im m\,(\omega_{3_2})$	–3.5490	0	3.3353	6.4713
$\Im m\,(\omega_{3_3})$	–6.2908	–3.1520	0	3.0184
$\Im m\,(\omega_{3_4})$	–8.6052	–5.8658	–2.9035	0

The global instability threshold is associated with the destabilisation of the first mode. It corresponds to the following critical Weber number:

$$W_{0_g}(R, \varepsilon) = W_a + \sqrt{\varepsilon}\, W_{2_1}(R) + O(\varepsilon^{3/4}). \tag{23}$$

The dependency of $W_{2_1}(R)$ with respect to R is shown in Figure 4.

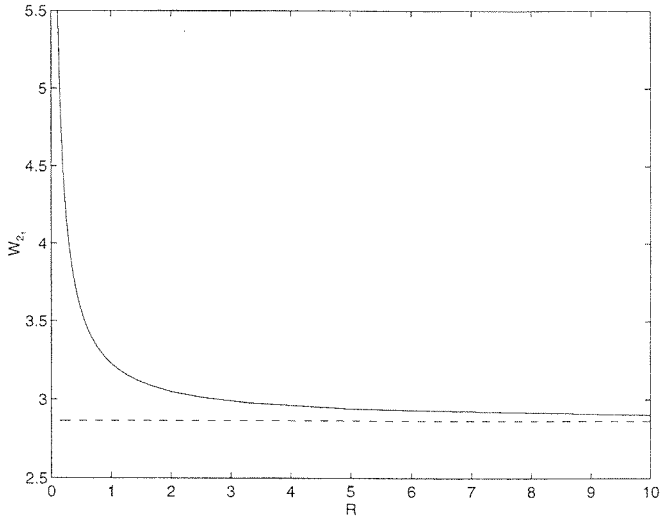

Fig. 4. – The critical parameter W_{2_1} versus the rescaled Reynolds number R. The dashed line corresponds to the asymptotic value for large Reynolds numbers.

At the global threshold, the size of the absolutely unstable region is calculated from the local dispersion relation (6). At leading order, the local absolute growth rate is evaluated by

$$\Im m\,[\omega_0(X, W_{0_g}, \mathrm{Re})] \sim c\,[W(X, W_{0_g}) - W_a]^{3/2} + \frac{\eta}{\mathrm{Re}}, \tag{24}$$

with

$$c \equiv -\frac{2\mu}{3}\sqrt{\frac{\mu}{3\lambda}} \approx 1.02948. \tag{25}$$

Using $W(X, W_{0_g}) - W_a \sim \sqrt{\varepsilon}\, W_{2_1}(R) - 3X/(2+W_a)$, the condition $\Im m\,(\omega_0(X)) \geq 0$ of absolute instability is satisfied for an interval ΔX given by:

$$\Delta X = \frac{(2+W_a)\sqrt{\varepsilon}}{3}\left[W_{2_1}(R) - \left|\frac{\eta}{cR}\right|^{2/3}\right]. \tag{26}$$

Figure 5 shows $\Delta X/\sqrt{\varepsilon}$ versus R.

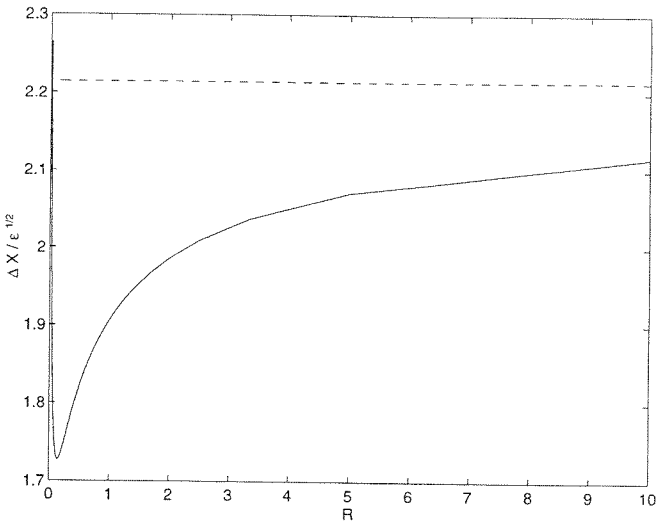

Fig. 5. – The length $\Delta X/\sqrt{\varepsilon}$ of the region of local absolute instability versus the rescaled Reynolds number R. The dashed line corresponds to the asymptotic value for large Reynolds number.

4.2. Application to a jet of water in air

When the fluids are given, the three control parameters are connected by the relation

$$\frac{\mathrm{Re}^4 W_0^3}{\varepsilon} = H \equiv \frac{\gamma^3}{\rho^3 \nu^4 g} \tag{27}$$

which is independent of the jet characteristics (radius and speed). Relation (27) implies that the parameter ε is a function of both W_0 and Re. Expression (23) must then be considered as an implicit equation for the critical Weber number W_{0_g}:

$$W_{0_g} = W_a + \frac{\mathrm{Re}^2 W_{0_g}^{3/2}}{\sqrt{H}}\, W_{2_1}\left(\frac{\mathrm{Re}^4 W_{0_g}^{9/4}}{H^{3/4}}\right). \tag{28}$$

The solution $W_{0_g}(\mathrm{Re})$ of the equation depends on the fluids considered via H. For the jet of water in air for which $H \approx 3.89 \times 10^{11}$, the result is represented in Figure 6.

Note the slope of the global transition curve: it is opposite to the slopes of the absolute/convective transition curve and of $W_{2_1}(R)$ (see *Fig.* 4). The apparent destabilising effect of viscosity is in fact due to the important variation of ε with respect to Re (*Fig.* 7).

Figure 7 shows that Re cannot exceed values larger than 200 without invalidating the weakly non-parallel flow assumption ($\varepsilon \ll 1$). Moreover, the Reynolds number cannot

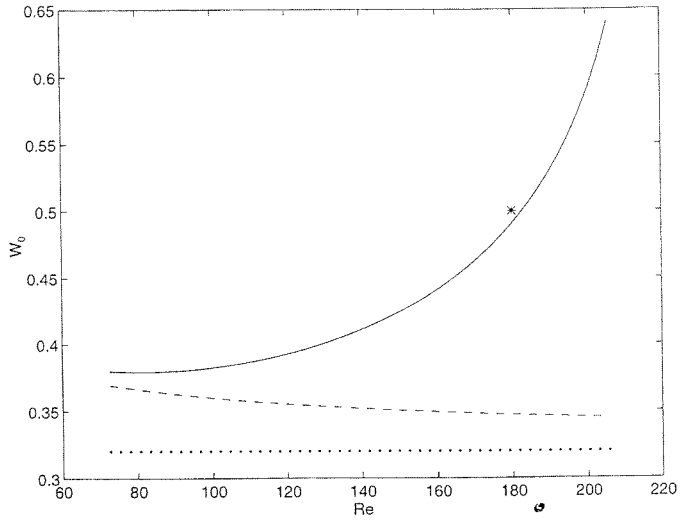

Fig. 6. – Critical Weber numbers for the jet of water in air versus the Reynolds number Re. Continuous line: the Weber number for the global transition. Dashed line: the Weber number for the local absolute/convective transition at the orifice. Dotted line: Asymptotic value for large Reynolds numbers for the local absolute/convective transition at the orifice. The star corresponds to the experimental data from Monkewitz (1990) for the transition to dripping in a jet of water in air from a circular orifice of radius 0.22 mm.

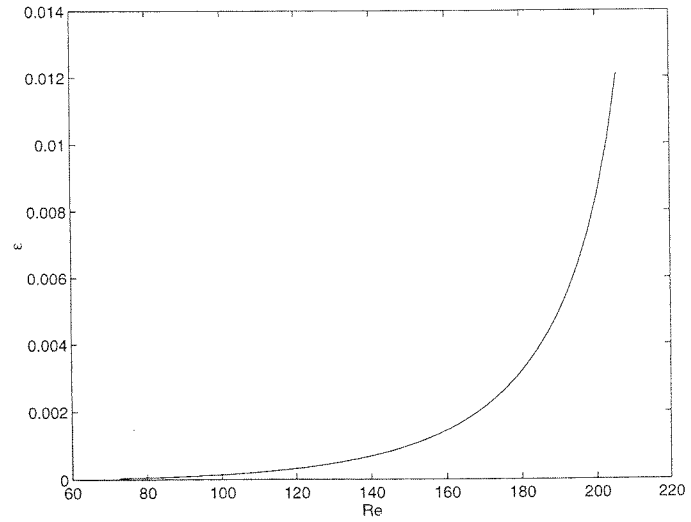

Fig. 7. – The parameter ε for the jet of water in air at the global transition versus the Reynolds number Re.

be too small without invalidating the non-viscous approximation. These two constraints explain the variation range of Re in Figure 6. Outside that range, the results are not expected to be accurate.

The transition to dripping has been experimentally studied on Monkewitz (1990). For a jet of water in air from a circular orifice of radius $R_0 \approx 0.22$ mm, he has obtained a transition to dripping for $W_0 \approx 0.5$ at $\mathrm{Re} \approx 180$. This point is displayed on Figure 6.

5. Conclusion

The falling capillary jet has been proved to be globally unstable above the local absolute/convective transition in qualitative agreement with the general mechanism described in Huerre and Monkewitz (1990) and with the conjecture of Monkewitz (1990). The critical Weber number for the global transition has been computed as a function of the Froude and Reynolds numbers when these two parameters are larger [*see* expression (23) and Figure 4]. The transition curve $W_{0_g}(\mathrm{Re})$ has been drawn for the special case of the jet of water in air (*Fig.* 6).

The global transition has been found to be of a new type. The global modes are composed of three local plane waves interacting at the orifice and their frequencies are given by expression (10a) which differs from the formula obtained by Monkewitz *et al.* (1993). The scalings are also different. The critical Weber number for the global transition is superior to the Weber number for the absolute/convective transition by a factor or order $\sqrt{\varepsilon}$, whereas the difference between both critical values was $O(\varepsilon^{2/3})$ in Monkewitz *et al.* (1993). Here, global growth rates are $O(\varepsilon^{3/4})$ for a control parameter $O(\varepsilon^{1/2})$ above threshold, they were larger $[O(\varepsilon^{2/3})]$ for a smaller value $[O(\varepsilon^{2/3})]$ in Monkewitz *et al.* (1993). Moreover, note also that the region of absolute instability necessary for global instability is also larger than in the other studies: compare $O(\sqrt{\varepsilon})$ in (26) with $O(\varepsilon^{2/3})$ in Chomaz *et al.* (1988) and Monkewitz *et al.* (1993).

It is argued that the global transition may correspond to the transition to dripping in the falling capillary jet. Below the global instability threshold, no temporally growing solution exists without being sustained by external noise. This global stability of the jet flow guarantees that the basic jet near the orifice is not affected by the rest of the flow. The jet does break up far downstream, as expected from the convective nature of the local instabilities: one indeed expects convected perturbations to reach a sufficiently large amplitude far downstream to be affected by the nonlinear effects that leads to breakup. This breakup can not be described by the present theory, and it is assumed that is does not influence the linear dynamics near the orifice. Above the global instability threshold, perturbations grow everywhere independently of external noise. In particular, they grow and modify the basic jet in the neighborhood of the orifice. If the destabilised global modes are not re-stabilised by nonlinear effects (subcritical bifurcation), these modifications could be important enough to explain the breakup of the jet into drops at the orifice, *i.e.* the transition to dripping. The experimental results for a jet of water in air by Monkewitz (1990) are in agreement with the interpretation but other data would be useful for confirmation.

APPENDIX

Resolution of the eigenvalue problem

This appendix deals with the resolution of the eigenvalue problem (14), (17a, b). Since only the eigenvalues are wanted, it is convenient to solve the adjoint eigenvalue problem which is defined by the same Eq. (14) and the following boundary conditions:

(29a) $$\Phi\,(u_0^*) = 0,$$

(29b) $$\Phi \underset{u\to+\infty}{\sim} \Phi_1^-,$$

where * denotes the complex conjugate, and Φ_1^- is the "balanced" formal asymptotic expansion near $+\infty$ of solutions of (14).

Three independent solution of (14) are given by the following integral representations:

(30) $$\Phi^{(k)} = \int_{\mathcal{C}_k} \exp\left(e^{-i\pi/8}\,us + e^{i\pi/4}\,\overline{W}_2\,\frac{s^2}{2} - \frac{s^4}{4}\right) ds, \quad k = 1,\,2,\,3.$$

where the complex contour $\mathcal{C}_k$ is composed of the two half-lines $(e^{i\,(k-1)\,\pi/2}\,\infty,\,0) \cup (0,\,e^{ik\pi/2}\,\infty)$ for all $k = 1, 2, 3$.

If $\Phi^{(k)}$ is written as

(31) $$\Phi^{(k)} = u^{1/3} \int_{\mathcal{C}_k} \exp\left(e^{i\pi/4}\,\overline{W}_2\,u^{2/3}\,\frac{r^2}{2}\right) \exp\left(u^{4/3}\,\Theta\,(r)\right) dr, \quad k = 1,\,2,\,3,$$

with

(32) $$\Theta\,(r) = e^{-i\pi/8}\,r - r^4/4,$$

the steepest descent method can be applied to determine the behavior of these solutions near infinity. Dominant contributions to integral (31) as $u \to \infty$ are invariably known to come from the stationary points of the function $\Theta\,(r)$, *i.e.* from the 3 roots of $\Theta'\,(r) = 0$ given by

(33) $$r_l = e^{-i\pi/24+2i\,(l-1)\,\pi/3}, \quad l = 1,\,2,\,3.$$

For large u, $\Phi^{(k)}$ is thus a linear combination of functions Φ_l^∞, $l = 1, 2, 3$ that correspond to the contributions from each r_l:

(34) $$\Phi_l^\infty \sim u^{-1/3} \exp\left(e^{i\pi/4}\,\overline{W}_2\,u^{2/3}\,\frac{r_l^2}{2}\right) \exp\left(u^{4/3}\,\Theta\,(r_l)\right) (a_l^{(0)} + a_l^{(1)}\,u^{2/3} + \cdots),$$

where

$$\Theta(r_l) = \frac{3}{4} e^{-i\pi/6+2i(l-1)\pi/3}. \tag{35}$$

From (34), it is clear that Φ_1^∞ is exponentially large, Φ_2^∞ oscillatory and Φ_3^∞ exponentially small so that Φ_2^∞ corresponds to the "balanced" formal asymptotic expansion Φ_1^- appearing in (29b). Consequently, condition (29b) means that the asymptotic expansion of the solution at $+\infty$ has a single contribution from the stationary point r_2.

The main idea is now to use this condition to choose the correct expression from the solution among the $\Phi^{(k)}$'s. Indeed, there is a single contribution from r_2 if and only if the integration contour $\mathcal{C}_k$ can be deformed into a streepest descent path that passes only through the stationary point r_2. Steepest descent paths are included in the stationary phase contours $\Im m\left[\Theta(r)\right] = \Im m\left[\Theta(r_l)\right]$. These contours together with the coutours $\Re e\left[\Theta(r)\right] = \Re e\left[\Theta(r_l)\right]$ are shown in Figure 8.

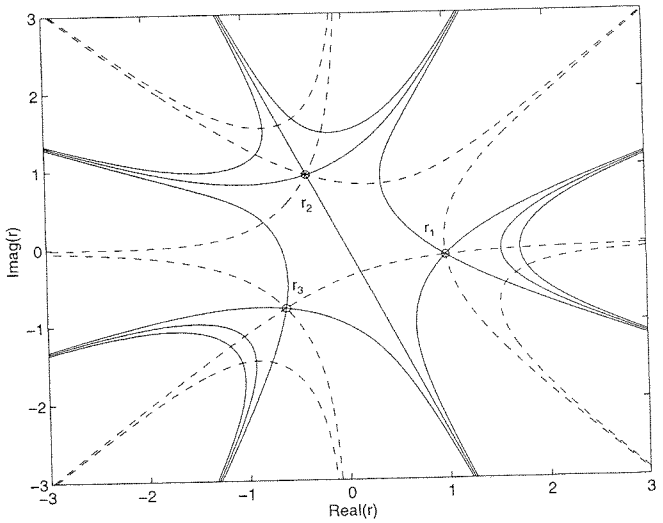

Fig. 8. – The function $\Theta(r)$ in the complex r-plane. Continuous lines: the contours $\Re e\left[\Theta(r)\right] = \Re e\left[\Theta(r_l)\right]$, $l = 1, 2, 3$. Dashed lines: the contours $\Im m\left[\Theta(r)\right] = \Im m\left[\Theta(r_l)\right]$, $l = 1, 2, 3$. The points r_l, $l = 1, 2, 3$ are the saddle points of the function Θ : $\partial_r \Theta(r_l) = 0$.

From this figure, one deduces that $\mathcal{C}_1$ is deformed to pass through the three stationnary points r_1, r_2 and r_3, $\mathcal{C}_2$ through r_2 and $\mathcal{C}_3$ through r_3. From the above argument, it finally results that the function $\Phi^{(2)}$ is the solution of (14) satisfying (29b). Note that the naive approach used here is rigorously justified in the more sophisticated framework of "resurgence" methods. The interested reader is referred to the textbook of Candelpergher *et al.* (1993) and in particular to pp. 45-49 where the asymptotic behavior of the Airy function in the complex plane is determined by "resurgence" methods.

The eigenvalue problem is now equivalent to finding the zeroes of $\Phi^{(2)}$. By contrast with the Airy functions, the zeroes of $\Phi^{(2)}$ are not tabulated and a numerical integration is

then necessary to fully solve the eigenvalue problem. The numerical procedure is simple because for $\overline{W}_2 = 0$, all the zeroes have an argument equal to $-5\pi/8$. For that value of $\overline{W}_2$, they are then given by $u = e^{-5i\pi/8}v$ where v is a positive real number that cancels

$$\int_0^{+\infty} \exp\left(\frac{\sqrt{2}}{2}vs - \frac{s^4}{4}\right) \cos\left(\frac{\sqrt{2}}{2}vs - \frac{\pi}{4}\right) ds.$$

The first zeroes are associated with

$$v_1 \approx 2.8868; \quad v_2 \approx 5.1523; \quad v_3 \approx 7.1303; \quad v_4 \approx 8.9404. \tag{36}$$

The evolution of the complex conjugates of these zeroes as $\overline{W}_2$ is progressively increased is shown in Figure 9.

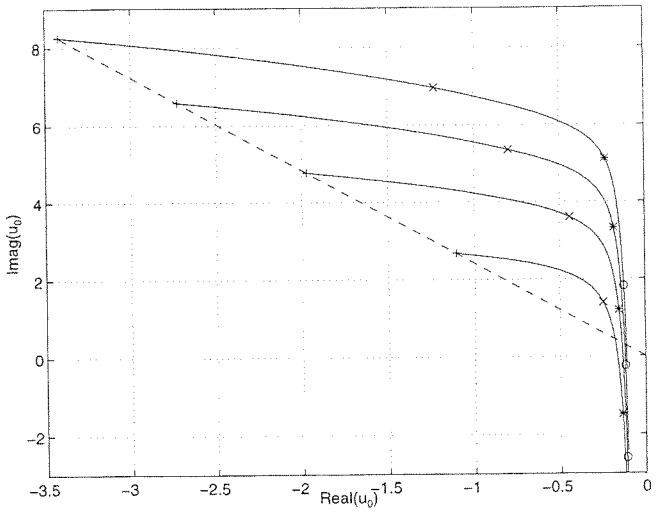

Fig. 9. – The trajectories of the complex conjugates of the first zeroes of the function $\Phi^{(2)}$ as $\overline{W}_2$ is varied. Symbols correspond to particular values of $\overline{W}_2$: '+' : $\overline{W}_2 = 0$; '×' : $\overline{W}_2 = 2.83$; '∗' : $\overline{W}_2 = 5.66$; 'o' : $\overline{W}_2 = 8.49$.

REFERENCES

BENDER C. M., ORSZAG S. A., 1978, *Advanced Mathematical Methods for Scientists and Engineers*, New York: McGraw-Hill.

BERS A., 1983, Space-time evolution of plasma instabilities-absolute and convective. In *Handbook in Plasma Physics* (ed. M. N. ROSENBLUTH and R. Z. SAGDEEV), **1**, Amsterdam: North-Holland, 451-518.

CANDELPERGHER B., NOSMAS J. C., PHAM T., 1993, *Approche de la résurgence*, Paris: Hermann.

CHANDRASEKHAR S., 1961, *Hydrodynamics and Hydromagnetic Stability*, New York: Dover.

CHOMAZ J. M., HUERRE P., REDEKOPP L. G., 1988, Bifurcations to local and global modes in spatially developing flows, *Phys. Rev. Lett.*, **60**, 25-28.

CHOMAZ J. M., HUERRE P., REDEKOPP L. G., 1991, A frequency selection criterion in spatially-developing flows, *Stud. Appl. Math.*, **84**, 119-144.

DESPRÈS T., 1992, Investivation of global instability in falling capillary jets. Report on a training period with P. A. MONKEWITZ, École Polytechnique, Palaiseau.

HUERRE P., MONKEWITZ P. A., 1990, Local and global instabilities in spatially developing flows, *Ann. Rev. Fluid Mech.*, **22**, 473-537.

KULIKOVSKII A. G., 1985, On the stability conditions for steady states and flows in regions extended in one direction. *Prikl. Mat. Mekh.*, **49**, 3, 411-418. [English translation: *J. Appl. Maths Mechs.*, **49**, 3, 316-321 (1985)].

LE DIZÈS S., HUERRE P., CHOMAZ J. M., MONKEWITZ P. A., 1996, Linear global modes in spatially-developing media. *Phil. Trans. R. Soc. Lond.* A, **354**, 169-212.

LE DIZÈS S., 1996, Global modes for the complex Ginzburg-Landau equation. To be published in *Proceedings of the Asymptotics in Mechanics conference*, St Petersburg, August 1944, A. H. NAYFEH and K. V. ROZHDESTVENSKY ed., 137-144.

LEIB S. J., GOLDSTEIN M. E., 1986a, The generation of capillary instabilities on a liquid jet, *J. FLuid Mech.*, **168**, 479-500.

LEIB S. J., GOLDSTEIN M. E., 1986b, Convective and absolute instability of a viscous liquid jet, *Phys. Fluids*, **29** (4), 952-954.

MONKEWITZ P. A., 1990, The role of absolute and convective instability in predicting the behavior of fluid systems, *Eur. J. Mech. B/Fluids*, **9**, 395-413.

MONKEWITZ P. A., HUERRE P., CHOMAZ J. M., 1993, Global linear stability analysis of weakly non parallel shear flows, *J. Fluid. Mech.*, **251**, 1-20.

LORD RAYLEIGH W. S., 1878, On the instability of jets. *Proc. Long. Math. Soc.*, **10**, 4-13.

YAKUBENKO P. A., 1997a, Capillary instability of an ideal jet of large but finite length. *Eur. J. Mech. B/Fluids*, **16**, 39-48.

YAKUBENKO P. A., 1997b, Global capillary instability of an inclined jet. Private communication. To be published in *J. Fluid Mech.*

(Manuscript received October 29, 1996;
accepted March 11, 1997.)